

## Phenothiazine Redox Active Conducting Polymer Films at Nanocomposite Surfaces

To cite this article: Brian Murphy *et al* 2020 *J. Electrochem. Soc.* **167** 027525

View the [article online](#) for updates and enhancements.

**Investigate your battery materials under defined force!**  
**The new PAT-Cell-Force, especially suitable for solid-state electrolytes!**



- Battery test cell for force adjustment and measurement, 0 to 1500 Newton (0-5.9 MPa at 18mm electrode diameter)
- Additional monitoring of gas pressure and temperature

[www.el-cell.com](http://www.el-cell.com) +49 (0) 40 79012 737 [sales@el-cell.com](mailto:sales@el-cell.com)

**EL-CELL**<sup>®</sup>  
electrochemical test equipment





## Phenothiazine Redox Active Conducting Polymer Films at Nanocomposite Surfaces

Brian Murphy,<sup>1</sup> Baljit Singh,<sup>2</sup> Aoife Delaney,<sup>1</sup> Susan Warren,<sup>3</sup> and Eithne Dempsey<sup>4,z</sup>

<sup>1</sup>Centre of Applied Science for Health (CASH), Technological University Dublin (TU Dublin)—Tallaght Campus, Dublin 24, Ireland

<sup>2</sup>MiCRA Biodiagnostics Technology Gateway, Technological University Dublin (TU Dublin), Tallaght Campus, Dublin 24, Ireland

<sup>3</sup>Technological University Dublin, City Centre Campus, Kevin Street, Centre for Research in Engineering Surface Technology (CREST), FOCAS Research Institute, Dublin 8, Ireland

<sup>4</sup>Department of Chemistry, Maynooth University, Maynooth Co. Kildare, Ireland

A redox active polymer based on phenothiazine (thionine) doped poly(3,4-ethylenedioxythiophene) PEDOT film was examined on a range of transducers (glassy carbon, Pt and screen printed electrodes). This was followed by investigations into the use of super activated carbon (SAC) and platinized super activated carbon (SAC-Pt) nanostructured electrode modifiers for enhanced polythionine/PEDOT film deposition. The Polythionine/PEDOT film was found to undergo a two-electron, two-proton (pH 1–4) or a two-electron, one-proton process (pH 4–8). Electrochemical investigations included scan rate studies confirming the surface confined behavior, with the most stable films (15% decrease in electroactivity) being evident at SPE modified with SAC-Pt—surface coverage ( $\Gamma$ )  $1.16 \times 10^{-10}$  mol cm<sup>-2</sup>. Surface morphology of the formed film was investigated via SEM/EDX and film hydrophobicity examined via contact angle measurements.

© 2020 The Electrochemical Society ("ECS"). Published on behalf of ECS by IOP Publishing Limited. [DOI: [10.1149/1945-7111/ab6a83](https://doi.org/10.1149/1945-7111/ab6a83)]

Manuscript submitted November 6, 2019; revised manuscript received January 2, 2020. Published January 23, 2020.

Phenothiazines are organic compounds that were first prepared by Bernthsen in 1883.<sup>1,2</sup> They are heterocyclic ring structures with the chemical formula  $S(C_6H_4)_2NH$ .<sup>3</sup> Traditionally, the synthesis of phenothiazine was performed by reacting diphenylamine and sulfur at temperatures of 250 °C but it was later discovered that the addition of small amounts of iodine would act as a catalyst, greatly reducing the temperature and the time of the reaction, leading to improved yields.<sup>1,4</sup> Preparation of phenothiazines can also be performed by thionation of diphenylamines and cyclization of diphenyl sulfides.<sup>2</sup> Phenothiazines have primarily been used for the treatment of psychotic diseases; however, they have many other therapeutic applications. The many derivatives of this group have been used as antihistamines, neuroleptics, antiparkinsonism and antiemetic agents.<sup>4,5</sup> Phenothiazines are metabolized in the body by various processes, mainly ring hydroxylation, ring sulphoxidation, N-demethylation and N-oxidation. It is understood that metabolites produced by these processes are responsible for the desired therapeutic effects observed.

Thionine (TH) also known, as Lauth's violet is one of the most studied phenothiazine amine derivatives and has primarily been used for biological staining. In its polymerized form, poly(thionine) (pTH) has received great interest as a stable redox polymer and can be used to mediate electron transfer in biosensors, particularly in the cases of H<sub>2</sub>O<sub>2</sub> and NADH.<sup>6</sup> An oligomeric layer can be formed following electrodeposition of thionine and Zhao et al. developed an ultrasensitive polythionine/AuNPs based dopamine sensor by modifying the surface of a GCE with pTH/AuNP composites. The pTH/AuNP/GCE could successfully detect dopamine over a linear range 7.5 to 320 nmol.L<sup>-1</sup> with LOD of 2.8 nmol.L<sup>-1</sup>.<sup>7</sup> Yang et al. recently reported the voltammetric detection of metronidazole on a 3D polythionine glassy carbon electrode<sup>8</sup> while label free DNA detection was achieved using poly(thionine) on glassy carbon and gold surfaces using charge perturbation.<sup>9</sup>

Karakin et al. have reported the proposed reaction mechanism for the electropolymerization of azines involving the formation of a cation-radical species after the release of one proton from the monomer at high positive potentials.<sup>10</sup> It was proposed by Schlereth and Karyakin that in the case of poly(thionine), monomer units could bind to the next monomer unit in the  $\alpha/\beta$  aromatic

position with respect to NH<sub>2</sub>.<sup>10,11</sup> Copolymerization of N-methylthionine with polyaniline was reported by Chen et al. and electrochromic and electrochemical properties of the novel material examined on ITO electrodes,<sup>12,13</sup> while new 2,5-di(2-thienyl)-1H-pyrrole derivatives were examined for their electrochemical and electrochromic properties with different phenothiazine groups.<sup>14</sup>

Poly(3,4-ethylenedioxythiophene) (PEDOT), a member of the poly(thiophene) (pTh) family, is considered to be the most successful pTh derivative due to its high electrical conductivity (0.4–400 S.cm<sup>-1</sup>) and chemical stability, thus showing great promise for biomedical applications and sensing.<sup>15–19</sup> Co-deposition of PEDOT/thionine films has been achieved in our group<sup>20,21</sup> enabling NADH detection and subsequently glutamate biosensing at Pt surfaces and more recently, using scanning electrochemical microscopy (SECM) to investigate PEDOT/thionine films for lactate detection.

Here we extend the growth of PEDOT/thionine films on underlying nanostructured materials based on super activated carbon—an adsorbent with good porosity and high surface area.<sup>22</sup> Activated carbons can be prepared from a variety of precursor materials, including coal, wood, bio waste and polymers<sup>23–25</sup> and have been used in a variety of applications such as gas storage, liquid phase adsorption and as carbon capacitors. These highly porous carbon structures are typically produced by chemical or physical activation. Once carbonization of the base material is performed, the internal porous structure is developed by thermal oxidation.<sup>23</sup> In comparison to activated carbons, super activated carbons (SAC) are prepared using KOH and NaOH for activation and give rise to unusually high surface areas.<sup>23,24</sup> Xia et al. demonstrated enhanced hydrogen storage at room temperature using super activated carbon, providing highly specific surface areas up to 2829 m<sup>2</sup> g<sup>-1</sup> with pore volumes of 2.34 cm<sup>3</sup> g<sup>-1</sup>. The material itself exhibited a hydrogen uptake of 0.95% wt at 298 K at 80 bar.<sup>25</sup> Platinised activated carbons have gained much attention in recent times due to their potential use in fuel cells.<sup>26</sup> Carbon materials have been used as catalytic supports for metals, such as platinum, due to the nature of their stability; porous structure and large surface area.<sup>27</sup> Bruno et al. deposited platinum nanoparticles on mesoporous carbon for use as a carbon-supported Pt catalyst. The catalyst was directly used in a methanol fuel-cell as a cathode catalyst and resulted in a 30% increase in energy density when compared to Pt supported on Vulcan carbon.<sup>28</sup>

<sup>z</sup>E-mail: [eithne.dempsey@mu.ie](mailto:eithne.dempsey@mu.ie)

The aim of this work is to examine the electrochemical polymerization and characterization of a conducting poly (3,4-ethylenedioxythiophene) film in the presence of thionine acetate at different conducting surfaces (GCE, Pt and SPE), both with and without SAC and Pt decorated SAC. The rationale for selection of SAC is based on its effectiveness as a support material for Pt nanoparticle decoration, allowing the influence of Pt particles on the redox film behavior to be considered. An electrochemical and surface characterization study followed with the view to examine film characteristics. Such nanocomposites have not previously, to the best of our knowledge been utilized as an underlying support layer for redox active film behavioral studies of this type, making possible the electropolymerization of thionine on Pt decorated carbon surfaces with superior film properties regarding stability and redox activity.

### Experimental

**Materials.**—3,4-Ethylene dioxythiophene (EDOT  $C_6H_6O_2S$  97% purity), thionine acetate ( $C_{12}H_9N_3S$ ), lithium perchlorate ( $LiClO_4$  98% purity), Hexachloroplatinic acid ( $H_2PtCl_6 \cdot 6H_2O$ ), Nafion<sup>®</sup>, phosphate buffered saline (PBS), hydrochloric acid ( $H_2SO_4$ ) were used as received from Sigma Aldrich, Vale Road, Arklow, Wicklow. Electrode inks—Dupont Inc. carbon conducting ink composites BQ242 were supplied by CCI Eurolam LTD, Ulmes Walton Lane, Leyland, Lancashire, United Kingdom and silver ink from the Gwent Group UK, Monmouth House, Mamhilad Park, United Kingdom. Polyethylene terephthalate (PET) materials, Melinex 339 (white), Melinex O and 3M adhesive materials were purchased from Cadillac Plastic Ltd, UK. Super activated carbon nanoparticle/nanopowder (SAC, <100 nm, Product 0530 HT) was purchased from Sky Spring Nanomaterials, Inc., Houston, USA. Deionised water (DI, 18 M $\Omega$ ) was used in all experiments.

**Instrumentation.**—All electrochemical synthesis and measurements were performed via the use of CH Instruments Inc. CH660C electrochemical potentiostat, 3700 Tennon Hill Drive Austin, TX 78738–5012, USA. A three-electrode system was used consisting of a working electrode, glassy carbon electrode (GCE area = 0.0707 cm<sup>2</sup>) or platinum (Pt area = 0.0314 cm<sup>2</sup>), an Ag/AgCl reference electrode and a platinum wire counter electrode (CH Instruments Inc.). Prior to use, working electrodes were vigorously polished in alumina slurries (1.0, 0.3 and 0.05  $\mu$ m) followed by rinsing with deionised water. Ag/AgCl reference electrodes were stored in a 3 M KCl solution when not in use. All electrochemical synthesis and measurements were performed at room temperature. Surface morphology of Polythionine/PEDOT modified SPEs were measured using SEM (JEOL 6390 IV) and hydrophobicity of the film was determined by First Ten Angstroms (FTA) Contact Angle and Surface Tension Analyzer, First Ten Angstroms, Inc., 465 Dinwiddie Street, Portsmouth, Virginia.

**Procedures.**—*Electrochemical deposition of polythionine/PEDOT modified electrodes.*—A monomer solution was prepared by fully dissolving 10 mM thionine acetate in 10 mM  $LiClO_4$  prior to the addition of 15 mM EDOT to the solution. Modified electrode films were formed by chronocoulometry by stepping the potential of the working electrode (Pt, GCE) from 0.0 V to +1.2 V vs Ag/AgCl until a charge of 5 mC was passed.<sup>21</sup> Modified electrodes were then vigorously rinsed with deionised water and placed in a beaker of stirred deionised water to assist in the removal of unreacted thionine monomer. Stabilization of the Polythionine/PEDOT film was performed by cycling in phosphate buffered saline (PBS) (pH 6) until stable currents were achieved.<sup>21</sup>

*Fabrication of screen printed electrodes.*—Screen Printed Electrodes (SPE) are miniaturized thick film electrodes used for electrochemical sensing<sup>29</sup> that were produced *in house*. The electrodes were comprised of a carbon based conducting ink product,

BQ242 supplied by DuPont Inc. in addition to a silver-based ink supplied from Gwent printed onto a PET substrate. Printing was performed using a DEK 248 screen printer, supplied by ASM Assembly Systems (DEK) 3975 lakefield Court, Suwanee, Georgia, 30024 USA and a removable screen outlining the three-track design. The carbon ink was applied to the surface of the screen and in turn the automated squeegee forced the ink across the surface of the screen, allowing for deposition onto the PET substrate in the shape of the desired three-track design. Once printing was completed, the PET substrate was removed and cured in an oven at 60 °C for 2 h. Cover slips were prepared by laser cutting and lamination techniques of a 3 M layer and a Melinex-O layer, which was then placed on the surface of the SPEs to give a defined electrode area of 2 mm<sup>2</sup>. Ag/AgCl Gwent ink was deposited onto the middle track of the three-track electrode for use as a reference electrode and cured for a further 1 h at 60 °C. Electrochemical measurements were facilitated by use of a DropSens SPE adaptor.

*Super activated carbon (SAC).*—An SEM image of the commercially available super activated carbon was recorded in house (JEOL JSM 6390 IV) (Fig. 1). The image demonstrate size, morphology and uniform distribution of super activated carbon nanoparticles (<100 nm—as per supplier information) used in this study.

*Platinum nanoparticle decoration of super activated carbon (SAC-Pt).*—Carbon materials are well reported to contain functional groups (–COOH, –C=O, –OH etc) which act as active sites in anchoring the nanoparticles. Any activation procedure (chemical functionalization or heat activation at higher temperatures) further increases the presence of such functional groups which means more active sites for nanoparticle decoration. As per supplier information, super activated carbon nanoparticles/nanopowder used in this study were subjected to heat treatment.

In a typical synthesis, the calculated amount (53.1 mg) of  $H_2PtCl_6 \cdot 6H_2O$  (20 mg Pt representing 20% (w/w) loading) was dissolved and stirred in 180 mL of deionised water. Super activated carbon nanopowder (SAC, 80 mg) in 90 ml of deionised water was dispersed via sonication for 10 min to achieve a homogeneous suspension, followed by addition of the hexachloroplatinic acid solution dropwise to the SAC solution using a dropping funnel and with continuous stirring.  $NaBH_4$  (0.6 M) in distilled water was maintained at 0 °C and then added to the mixed solution and stirred for 30 min. The solution was centrifuged followed by washing with deionised water until all chloride ions were removed, as confirmed by the silver nitrate test. The sample was then dried in a vacuum at 100 °C (overnight).

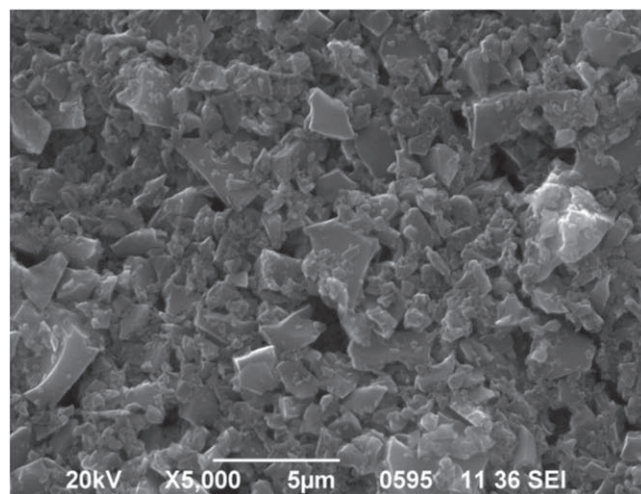


**Figure 1.** SEM image of super activated carbon nanoparticles (SAC) scale bar 5  $\mu$ m.

**Electrode fabrication.**—Super activated carbon (SAC) and platinumised SAC (SAC-Pt) solutions were prepared by dissolving 3 mg of SAC or SAC-Pt in 1 mL of water isopropyl alcohol mixture (3:1). The calculated amount of Nafion® solution (1%, v/v, diluted from the 5% Nafion® solution) was added to the dispersion, by maintaining the SAC materials (SAC and SAC-Pt) to Nafion® ratio at 8:1. The mixture was sonicated in order to achieve a uniform solution. SAC and SAC- modified electrodes were prepared by dispensing 20  $\mu\text{L}$  of SAC or SAC-Pt solutions onto the surface of the electrodes and cured at 60 °C in an oven until dry. (see surface analysis section for SEM images).

Prior to SEM/EDX analysis, modified SPEs were loaded onto an aluminum stub and fixed to the surface with aluminum tape to ensure

a good conductive path was achieved and to aid in the draining of electrons from the surface of the samples, preventing sample charging).

## Results and Discussion

**Electrochemical deposition of polythionine/PEDOT film on GCE.**—A cyclic voltammogram showing the introduction of thionine into a PEDOT film is shown in Fig. 2. polymerization was performed by cyclic voltammetry for 20 cycles over the potential window  $-0.5\text{ V}$  to  $+1.2\text{ V}$  at a scan rate of  $0.1\text{ V}\cdot\text{s}^{-1}$  vs Ag/AgCl from a solution containing 10 mM thionine, 15 mM EDOT and 10 mM  $\text{LiClO}_4$ . The deposition curve shows the presence of a redox

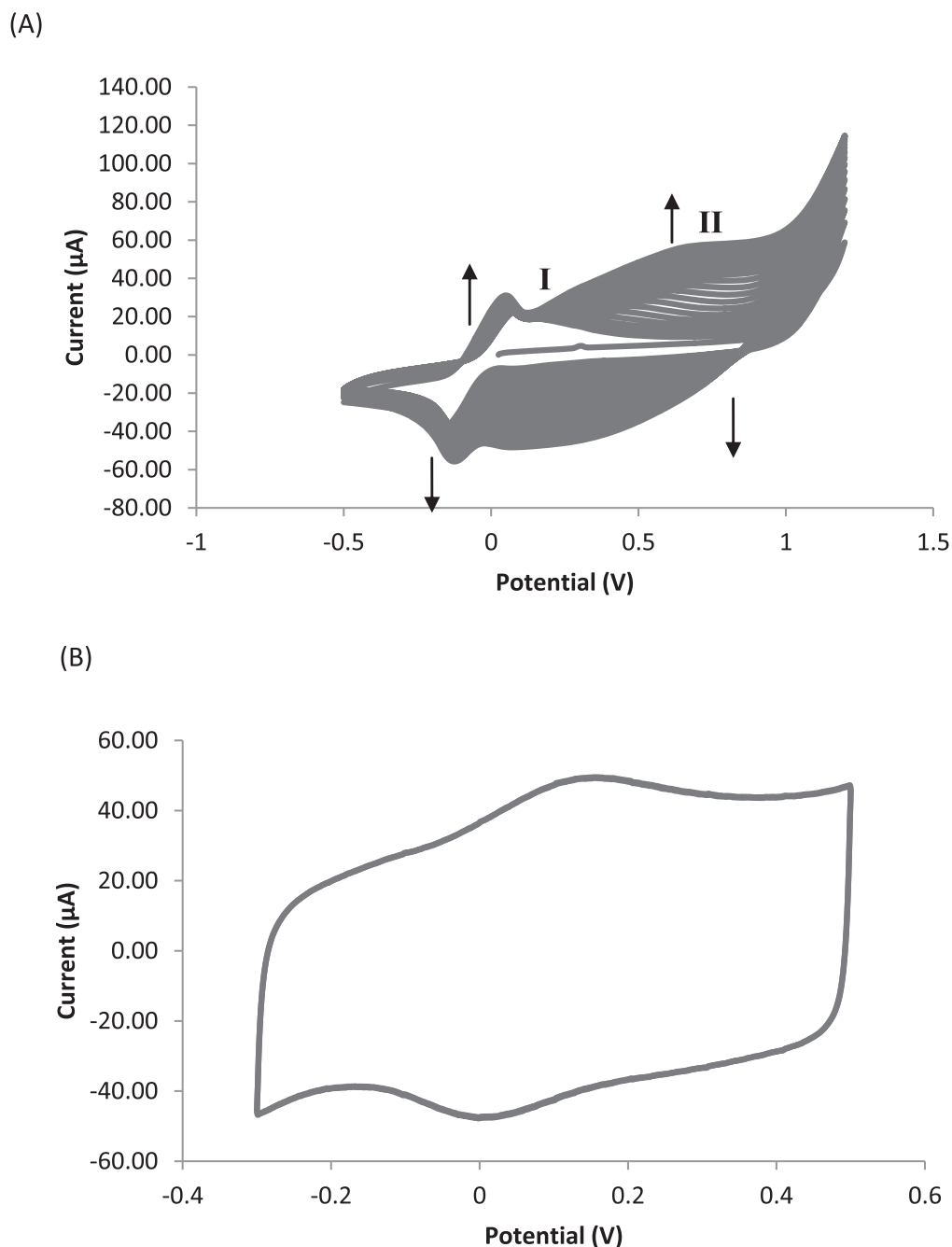


**Figure 2.** (a) Cyclic voltammograms showing Polythionine/PEDOT deposition from solution containing 10 mM thionine, 15 mM EDOT in 10 mM  $\text{LiClO}_4$  at a scan rate  $0.1\text{ V}\cdot\text{s}^{-1}$  vs Ag/AgCl at GCE electrode. The cyclic voltammogram shows peak (I) corresponding to thionine polymerization and (II) corresponding to EDOT polymerization. (b) Cyclic voltammogram for the final cycle of a stabilized Polythionine/PEDOT film PBS (pH 6) at a scan rate  $0.1\text{ V}\cdot\text{s}^{-1}$  vs Ag/AgCl at GCE.  $E_{p(\text{ox})}$  0.155 V,  $E_{p(\text{red})}$   $-0.001\text{ V}$ ,  $\Delta E_p$  (0.156 V). Surface coverage ( $\Gamma$ ) =  $1.03 \times 10^{-9}\text{ mol}\cdot\text{cm}^{-2}$ .

couple close to 0 V vs Ag/AgCl (peak I) which is a result of thionine being introduced during the anodic polymerization of PEDOT (peak II).<sup>21</sup> During electropolymerization the initial anodic sweep creates a radical cation via  $1 e^-$  oxidation of the thionine monomer which is followed by delocalization, producing an electrophilic site at the ortho position on the aromatic ring, allowing radical dimerization via C–N coupling. This process results in a mixture of linked species in a manner similar to aniline polymerization.<sup>10</sup>

As reported previously, electrodeposition of thionine may be facilitated via copolymerization of EDOT, generating a redox active film with improved characteristics (in terms of stability and operating potential  $E_{1/2} = 0.005$  V vs Ag/AgCl), enabling direct deposition onto Pt transducers, which is not possible in the case of thionine alone.<sup>21</sup> The broad reduction and oxidation waves, superimposed on the PEDOT conducting polymer background current indicate the possibility of thionine—EDOT (S–S) interactions and/or cation- $\pi$  interactions.<sup>30</sup> The resulting film was then cycled in PBS

(pH 6) for 20 cycles with the final cycle shown in Fig. 2b, resulting in a 23% decrease in electroactivity upon cycling.

*Electrochemical deposition of polythionine/PEDOT film at Pt electrode.*—The cyclic voltammogram for the polymerization of the Polythionine/PEDOT film on a Pt electrode is presented in Fig. 3a. polymerization was performed by cyclic voltammetry for 20 cycles over the potential window  $-0.5$  V to  $+1.2$  V at a scan rate of  $0.1 \text{ V}\cdot\text{s}^{-1}$  vs Ag/AgCl from a solution containing 10 mM thionine acetate, 15 mM EDOT and 10 mM  $\text{LiClO}_4$ . The resulting film shows is similar to that formed at GCE, albeit with a less evident redox couple. The film was then cycled in PBS (pH 6) for 20 cycles with a 32% decrease in electroactivity upon cycling.

When comparing the Polythionine/PEDOT deposition curve at a bare screen printed electrode (data not shown), relative to a GCE and Pt, thionine polymerization (peak I) appeared less sharp/prominent relative to polymerization at a GCE or Pt. Following deposition, the

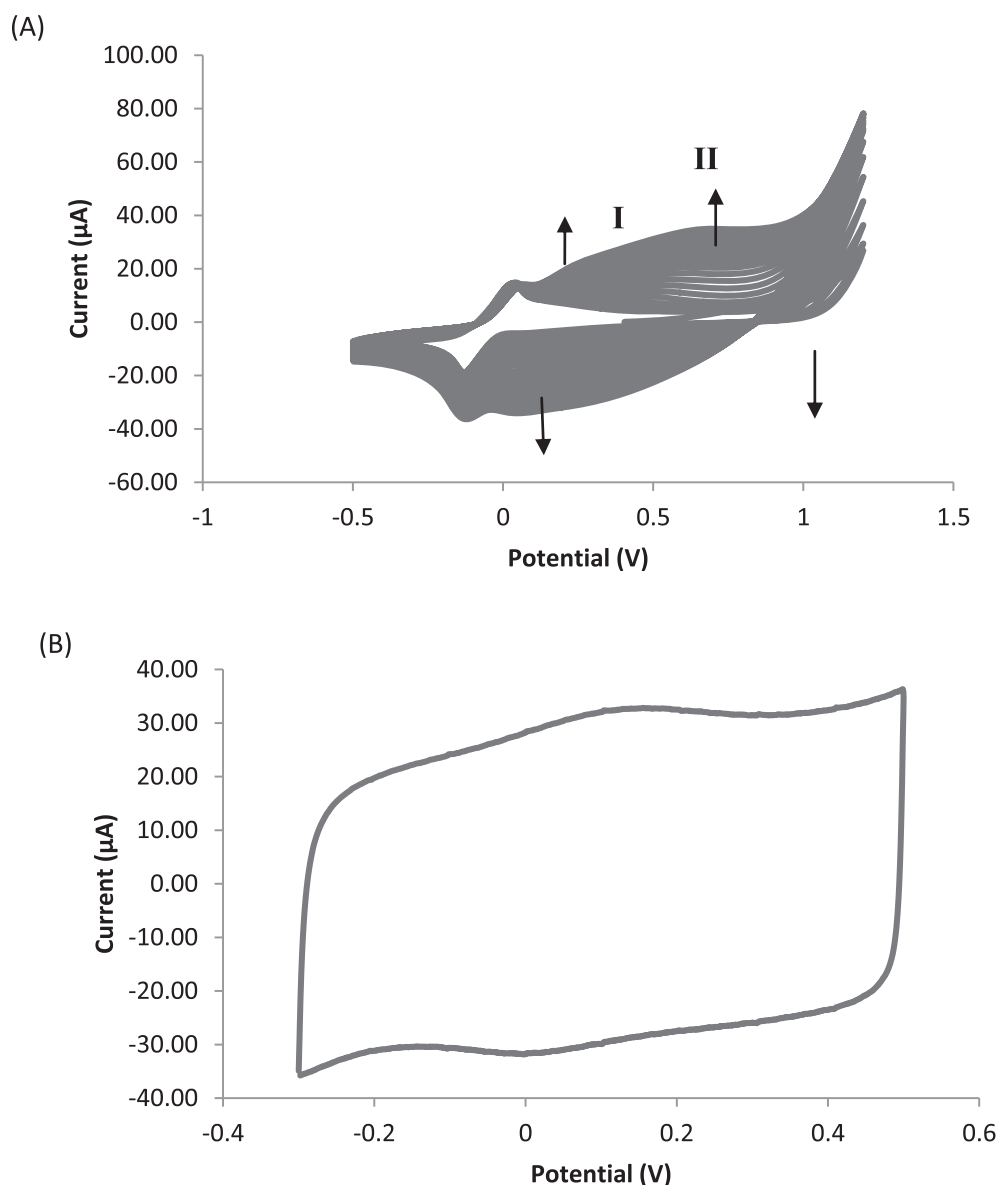


**Figure 3.** (a) Cyclic voltammograms showing Polythionine/PEDOT deposition from solution containing 10 mM thionine, 15 mM EDOT in 10 mM  $\text{LiClO}_4$  at a scan rate  $0.1 \text{ V}\cdot\text{s}^{-1}$  vs Ag/AgCl at Pt macro electrode. The cyclic voltammogram shows peak (I) corresponding to thionine polymerization and (II) corresponding to EDOT polymerization. (b) Cyclic voltammogram for the final cycle of a stabilized Polythionine/PEDOT film in PBS (pH 6) at a scan rate  $0.1 \text{ V}\cdot\text{s}^{-1}$  vs Ag/AgCl at Pt.  $E_{p(\text{ox})} 0.157$  V,  $E_{p(\text{red})} -0.002$  V,  $\Delta E_p (0.159$  V). Surface coverage ( $\Gamma$ ) =  $5.90 \times 10^{-10} \text{ mol}\cdot\text{cm}^{-2}$ .

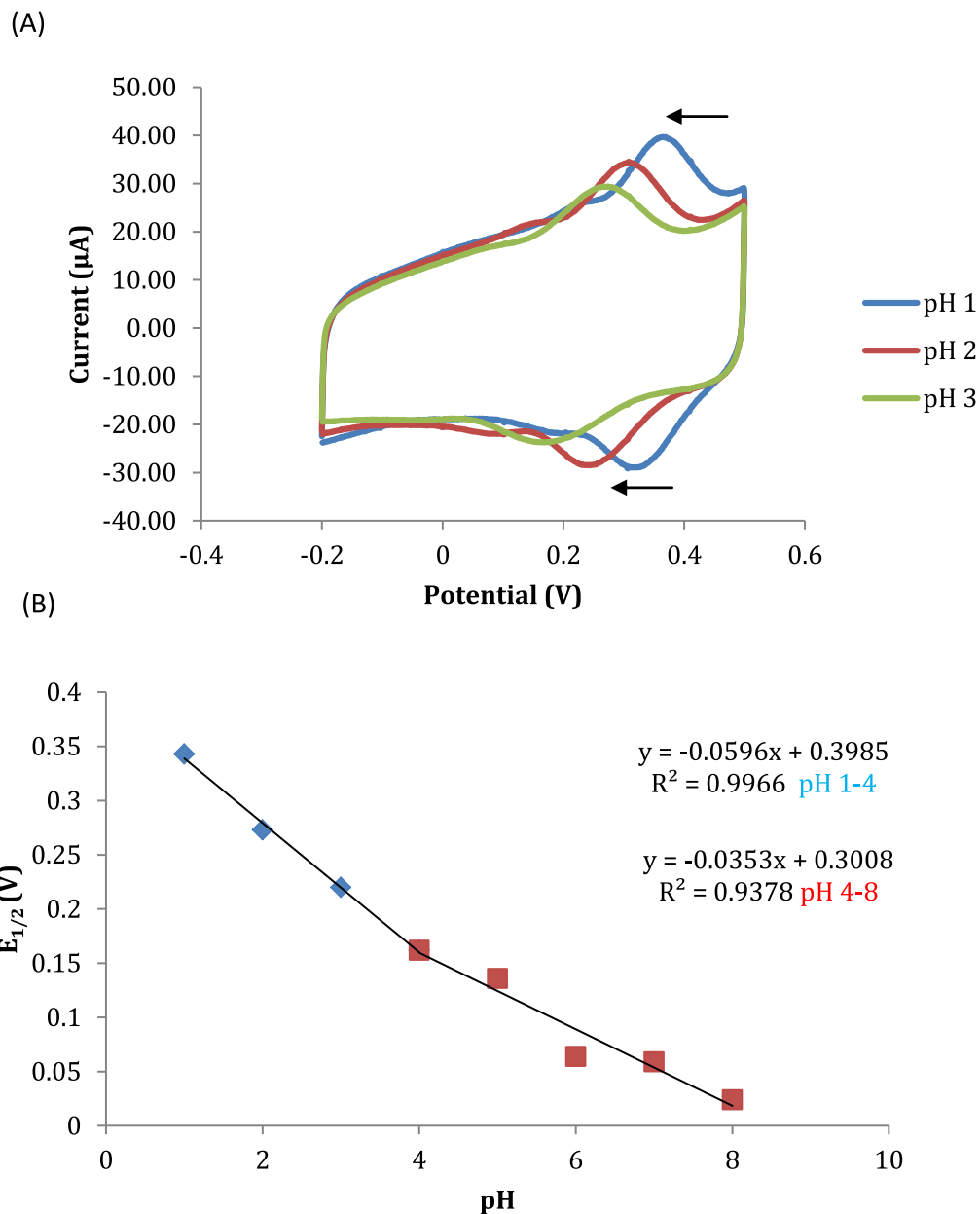


**Figure 4.** (a) Cyclic voltammograms showing cathodic shift in peak position of the Polythionine/PEDOT film at Pt transducer with increasing pH. (b) Plot of  $E_{1/2}$  vs pH for Polythionine/PEDOT film obtained via cyclic voltammetry at  $0.005 \text{ V.s}^{-1}$  over the pH range 1–8 from a solution containing 10 mM thionine, 15 mM EDOT, 10 mM  $\text{LiClO}_4$ .

resulting film was then cycled in PBS (pH 6) for 20 cycles with a 15% decrease in electroactivity upon cycling, being the most stable film formed relative to GCE (23%) and Pt (32%). Surface coverage values ( $\Gamma$ ) ( $\text{mol.cm}^{-2}$ ) were  $1.03 \times 10^{-9}$  (GCE/polythionine/PEDOT),  $5.9 \times 10^{-10}$  (Pt/polythionine/PEDOT), and  $5.94 \times 10^{-10}$  (SPE/polythionine/PEDOT).

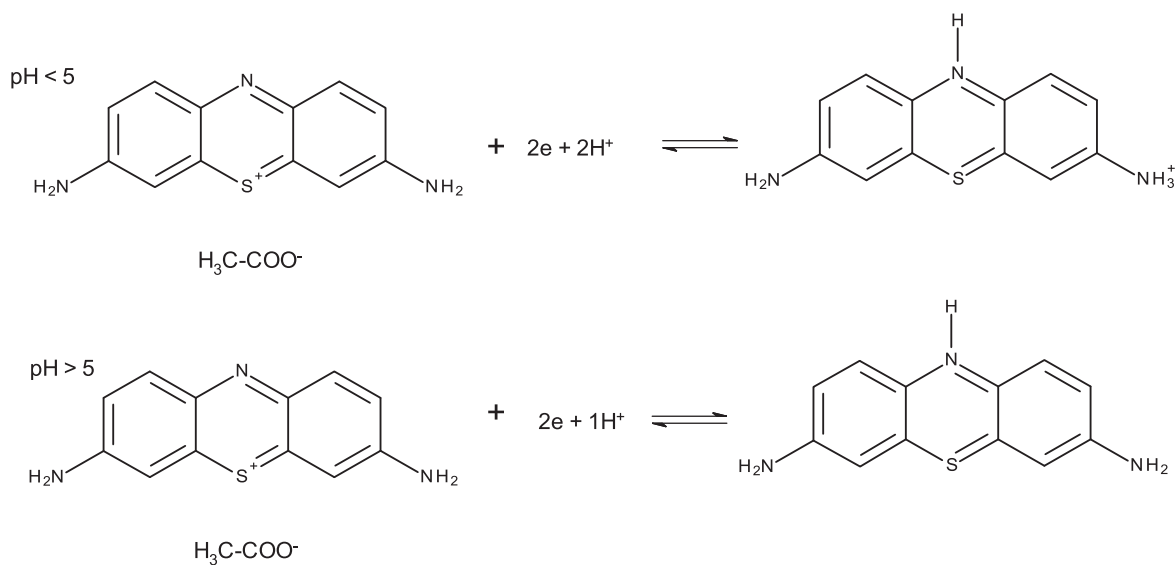
The effect of pH on the Polythionine/PEDOT film at a Pt electrode was investigated over the pH range 1–8 using cyclic voltammetry (Fig. 4). The effect of pH on the  $\Delta E_p$  of phenothiazine dyes has been previously investigated showing that with increasing pH, reduction of these dyes is less favorable as protonation of the heterocyclic nitrogen becomes more difficult<sup>31</sup> (see Scheme 1). As pH was increased from pH 1.0–4.0, the  $E_{1/2}$  for the thionine oxidation/reduction process shifted towards a more negative potential (more protons allowing more facile reduction of the thionine film). From pH 4.0–8.0, further  $E_{1/2}$  shifts were observed resulting in the formation of two regions of differing slopes. For pH 1.0–4.0 a

slope of  $59.6 \text{ mV.pH}^{-1}$  was observed indicating a two-electron, two-proton process, while for pH 4.0–8.0 a slope of  $35.3 \text{ mV.pH}^{-1}$  was observed indicating a two-electron, one-proton process as stated in the literature.<sup>32</sup> The intersection of the two linear sections at approximately pH 4.0 would suggest that the  $\text{pK}_a$  of deposited Polythionine/PEDOT film was 4.0, close to the literature value of 5.0 for surface deposited thionine alone.<sup>33</sup>

The expression below shows the relationship between  $E_p$  and pH where  $\Delta E_p$  is the change in peak potential,  $\Delta \text{pH}$  is the change in pH,  $m$  is the number of protons and  $n$  is the number of electrons.

$$\frac{\Delta E_p}{\Delta \text{pH}} = \frac{m}{n} 0.059 \text{ V}$$

**Polythionine/PEDOT scan rate studies.**—The effect of scan rate on peak current of the Polythionine/PEDOT film (grown on GCE



**Scheme 1.** Proposed reaction scheme for the two-electron, two-proton reaction of thionine over the pH range 1–4 and a two-electron, one-proton reaction over the pH range 4–8.

and Pt electrodes) was investigated by varying the scan rate from  $0.005 - 1.0 \text{ V.s}^{-1}$  in 0.01 M PBS (pH 6) for both a GCE and Pt macro electrode as shown in Fig. 5a. A plot of peak current ( $I_p$ ) vs scan rate ( $\text{V.s}^{-1}$ ) is shown in Fig. 5b with the linear correlation verifying that the redox process was surface confined. As  $\nu$  increased the film peak to peak separation also increased suggesting a kinetic limitation to charge transfer in the loaded PEDOT film. A plot of  $\text{Log } I_p$  vs  $\text{Log scan rate}$  for Polythionine/PEDOT film at GCE resulted in a slope of 0.9056 (close to the ideal value of 1) confirming the adsorbed surface confined film. Further studies of the Polythionine/PEDOT film were performed at a platinum electrode with current vs scan rate relationship being linear up to  $1 \text{ V s}^{-1}$  with the  $\text{log } I_p$  vs  $\text{log } \nu$  plot resulting in a slope of 0.97. The slope of Laviron plots resulted in  $\alpha = 0.43$  for the anodic process with apparent charge transfer rate constant  $k_s$  of  $1.35 \times 10^{-3} \text{ s}$ .

**Polythionine/PEDOT growth at SAC and SAC-Pt modified surfaces.**—GCE, Pt and carbon SPE were modified with (i) super activated carbon (SAC) and (ii) platinised SAC (SAC-Pt) in order to assess the influence of increased surface area to volume ratio and measure the conductivity/catalytic effects. The surface of the GCE and Pt electrode was modified by dispensing  $20 \mu\text{L}$  of SAC or SAC-Pt ( $3 \text{ mg.mL}^{-1}$  in 1% Nafion<sup>®</sup> solution consisting of 3:1 water: IPA) onto the electrode surface followed by drying in an oven at  $60^\circ\text{C}$ . Modification of the SPE was performed by dispensing  $5 \mu\text{L}$  of SAC or SAC-Pt onto the working electrode surface. In order to control polymer thickness via quantity of charge passed, electrodeposition of the Polythionine/PEDOT film was subsequently performed via chronocoulometry by stepping the potential from 0.0 V to +1.2 V until 5 mC of charge had passed, followed by stabilization in PBS (pH 6) for 20 cycles.

Figure 6A illustrates Polythionine/PEDOT deposition at a SAC modified GCE via chronocoulometry. Figure 6B illustrates the effect of SAC on the Polythionine/PEDOT film on a GCE. The enhanced current response at the GCE/SAC/pTH-PEDOT electrode in comparison to the GCE/SAC background was evident, confirming that the Polythionine/PEDOT film was successfully polymerized onto the GCE/SAC surface. The presence of SAC promoted film growth with provision of a highly porous structure with a large specific surface area, thus providing a platform for increased Polythionine/PEDOT film growth sites.<sup>22,34</sup> When comparing the results obtained in Fig. 6 to that of Fig. 2, it was determined that Polythionine/PEDOT deposition, in the presence of SAC, resulted in a 90 mV cathodic shift in oxidation peak

potential indicating more facile electron transfer at the nanostructured surface.

The influence of SAC-Pt on Polythionine/PEDOT growth at a GCE is presented in Fig. 7. with films formed via chronocoulometry and stabilized by potential cycling. As expected, an increase in current was observed at 0.073 V for the GCE/SAC-Pt/pTH-PEDOT signal over that of the GCE/SAC-Pt background signal alone, confirming that the Polythionine/PEDOT film was successfully polymerized onto the surface of GCE/SAC-Pt modified electrode. The effect of SAC and SAC-Pt on Polythionine/PEDOT film growth was compared to that of film polymerized on an unmodified GCE. Figure 7 illustrates that Polythionine/PEDOT in the presence of SAC or SAC-Pt influenced the surface coverage with a doubling of  $\Gamma$  values obtained (Table I) when compared to films growth in their absence. The presence of platinised SAC further promote Polythionine/PEDOT deposition in comparison to SAC alone, possibly due to a combination of a large surface area with dispersed Pt nanoparticles on the carbon support facilitating growth sites for the redox and conducting polymer film formation.

Figure 8 illustrates the effect of SAC on Polythionine/PEDOT film growth via chronocoulometry at a Pt electrode. Resultant films were compared and enhanced current was evident in the case of the Pt/SAC/pTH-PEDOT in comparison to the Pt/SAC background. The Polythionine/PEDOT film grown at a bare Pt (Fig. 3) was compared with that of a Pt/SAC modified electrode (Fig. 8) and the presence of SAC resulted in a 56 mV cathodic shift of the oxidation wave for the Polythionine/PEDOT film. The influence of SAC and SAC-Pt on Polythionine/PEDOT film growth at SPEs relative to films polymerized at unmodified SPE resulted in greater surface coverage values  $-3.91 \times 10^{-11} \text{ mol cm}^{-2}$  (bare SPE)  $5.39 \times 10^{-11} \text{ mol cm}^{-2}$  (SPE/SAC/pTH-PEDOT) and  $1.16 \times 10^{-10} \text{ mol cm}^{-2}$  (SPE/SAC-Pt/pTH-PEDOT) (see data Table I).

The effect of SAC and SAC-Pt on Polythionine/PEDOT deposition at a GCE, Pt and SPE was investigated and the Polythionine/PEDOT film deposition in the presence of SAC or SAC-Pt led to changes in  $E_{p(\text{ox})}$  and  $E_{p(\text{red})}$  values as well as increases in film surface coverage (see Table I for summary electrochemical data). Overall, the use of SAC-Pt leads to increased surface coverage in comparison to SAC alone suggesting that SAC-Pt accelerates Polythionine/PEDOT film deposition on the transducer examined. Smaller peak to peak separation ( $\Delta E_p$ ) values were evident upon film deposition in the presence of SAC/SAC-Pt and cathodic shifts in  $E_{1/2}$  indicated stabilization of the oxidized state of polythionine possibly due to electron donating effects at the heterogeneous

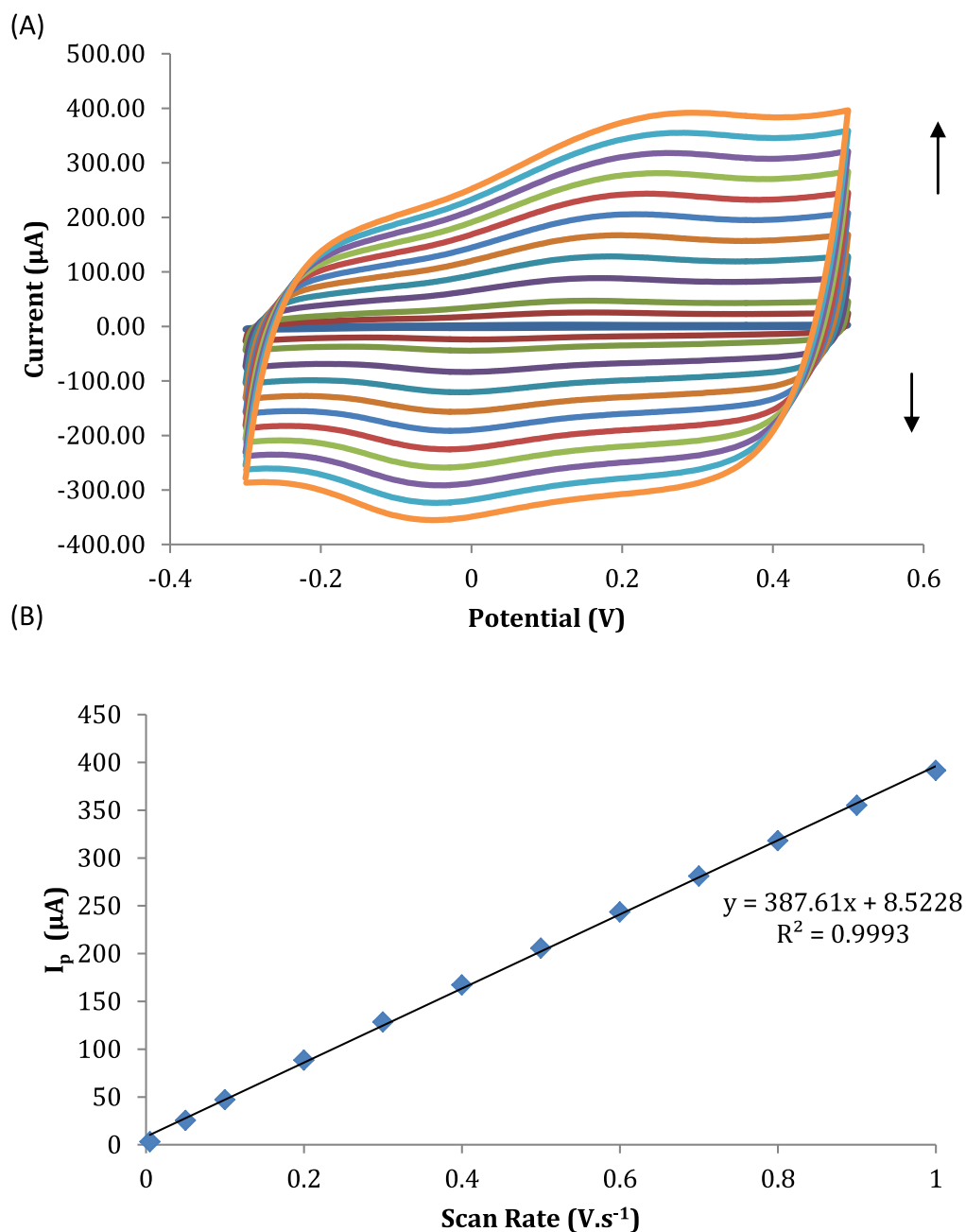


**Figure 5.** (a) Scan rate study for cyclic voltammograms ( $0.005$  to  $1.0 \text{ V}\cdot\text{s}^{-1}$ ) of the Polythionine/PEDOT film performed in PBS (pH 6) at a GCE electrode. (b) Peak current ( $I_p$ ) vs scan rate ( $\text{V}\cdot\text{s}^{-1}$ ) for Polythionine/PEDOT film formed from a solution of 10 mM thionine, 15 mM EDOT, 10 mM  $\text{LiClO}_4$  at GCE electrode. Surface coverage ( $\Gamma$ ) =  $1.45 \times 10^{-3} \text{ mol}\cdot\text{cm}^{-2}$ .

activated carbon surface. Enhanced film stability and significant increases in surface coverage were also evident indicating that greater film loading was possible at these nanostructured surfaces.

**Surface analysis.**—Scanning electron micrographs (SEM) of the carbon SPEs were performed to identify changes to surface morphology of the SPEs when modified with SAC-Pt and SAC-Pt/pTH-PEDOT. Energy dispersive X-ray images were performed with each modification for elemental characterization. Figure 9A illustrates the SEM image obtained for a bare carbon SPE. The surface appears ridged in structure with particles varying in diameter. The resulting EDX spectra show the presence of carbon only as expected. Figure 9B SEM image of the carbon SPE after modification with SAC-Pt. The surface morphology of the SPE appears to have been structurally modified. The structure of the surface appears much

more granular with long clustered chains visible. The accompanying EDX spectra provides elemental analysis of the surface and identifies the presence of SAC-Pt as there is an increased response for carbon as well as a response for platinum as expected. The presence of oxygen, fluorine and sulfur peaks can be explained as the SAC-Pt solution is prepared in 1% Nafion<sup>®</sup>, which contains said elements. Figure 9C is the resulting SEM image of a carbon SPE after modification with both SAC-Pt and Polythionine/PEDOT polymerized film. The addition of the Polythionine/PEDOT film resulted in a change to surface morphology with the presence of dense defined ridges, which appear to house granular clusters in between. EDX analysis identifies the presence of the Polythionine/PEDOT film, as there was an increased response for sulfur, which was present in both thionine and PEDOT respectively but also the presence of nitrogen, present in the structure of thionine.



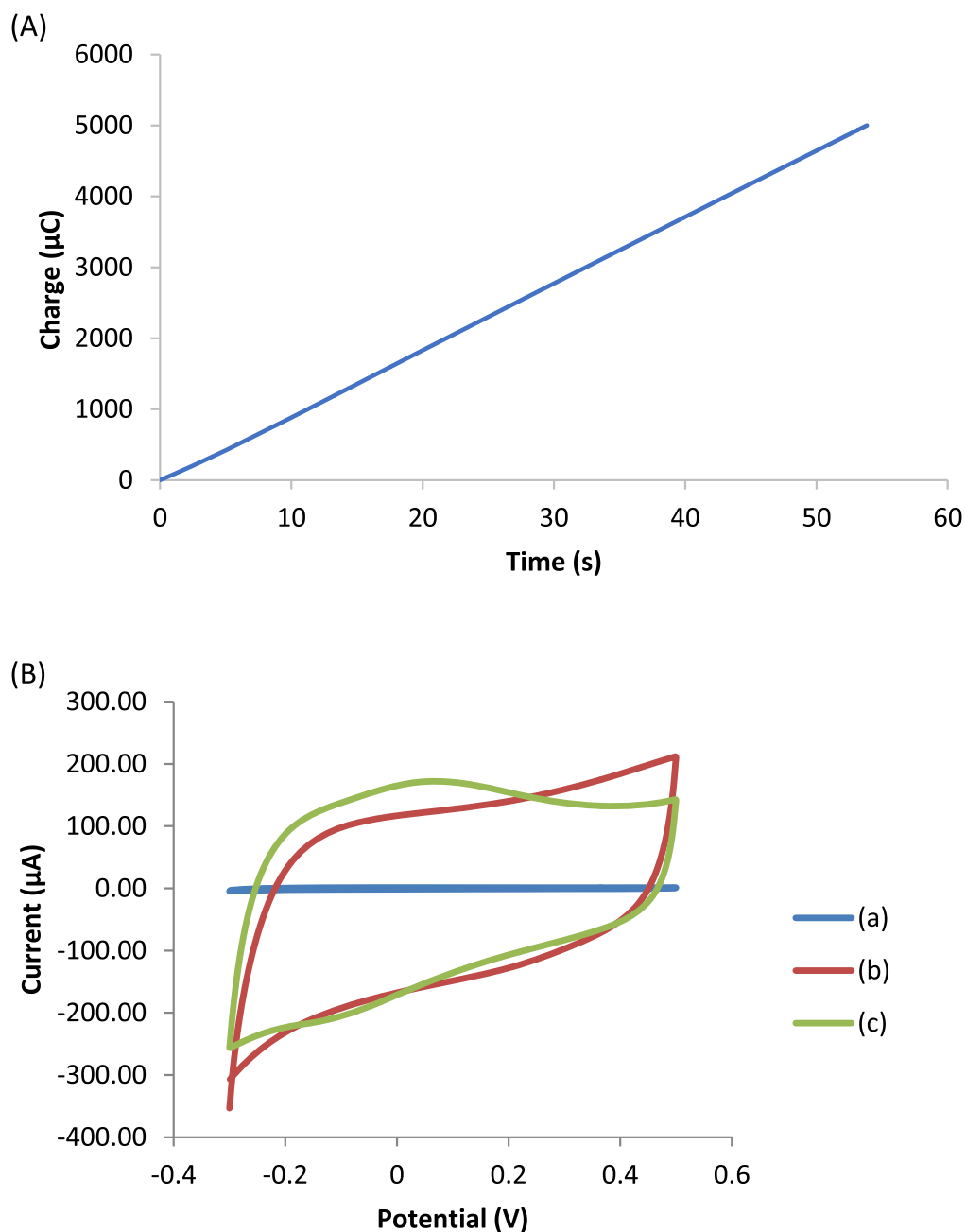


**Figure 6.** (A) Polythionine/PEDOT deposition by chronocoulometry from a solution containing 10 mM thionine, 15 mM EDOT, 10 mM LiClO<sub>4</sub> vs Ag/AgCl at SAC modified GCE electrode. (B) Cyclic voltammogram showing Polythionine/PEDOT following deposition from solution containing 10 mM thionine, 15 mM EDOT, 10 mM LiClO<sub>4</sub> at scan rate 0.1 V.s<sup>-1</sup> vs Ag/AgCl at a SAC modified GCE electrode. (a) GCE, (b) GCE/SAC, (c) GCE/SAC/pTH-PEDOT,  $E_{p(ox)} = 0.0644$  V,  $E_{p(red)} = -0.096$  V,  $\Delta E_p = 0.161$  V. pTH-PEDOT surface coverage ( $\Gamma$ ) =  $2.22 \times 10^{-9}$  mol.cm<sup>-2</sup>.

**Contact angle measurements.**—Surface hydrophilicity of the Polythionine/PEDOT film was measured using the FTA Contact Angle and Surface Tension Analyzer. Polythionine/PEDOT films were prepared by chronocoulometry as previously stated on carbon SPEs. A single water droplet (50 μL) was manually dispensed from the micrometer syringe onto the surface of the Polythionine/PEDOT film. Using the FTA 32 software, a static snapshot was taken by the optical camera of the dispensed droplet on the surface of the Polythionine/PEDOT film analyzing the change in contact angle relative to the SPE surface prior to Polythionine/PEDOT deposition (ESM 1). When comparing the average contact angle for the control SPEs a value of 87.33° (n = 5, S.D 3.28) was observed, confirming that the control SPEs (unmodified) are slightly hydrophilic. Following electrodeposition of the Polythionine/PEDOT film onto

the surface of the SPEs the average contact angle decreased to 68.30° (n = 5 s.D. 2.05) confirming that the presence of Polythionine/PEDOT film resulted in a more hydrophilic surface.

### Conclusions

The electrochemical deposition of the Polythionine/PEDOT film was successfully deposited onto the surface of GCE, Pt and SPEs. It was determined that films deposited on GCE and SPE showed greater film stability in comparison to that of films grown on a Pt electrode. The effect of pH on the Polythionine/PEDOT film was measured and in acidic conditions, the film underwent a two-electron, two-proton reaction; while at a more basic pH the film underwent a two-electron, one-proton process (slopes of  $E_p$  vs pH

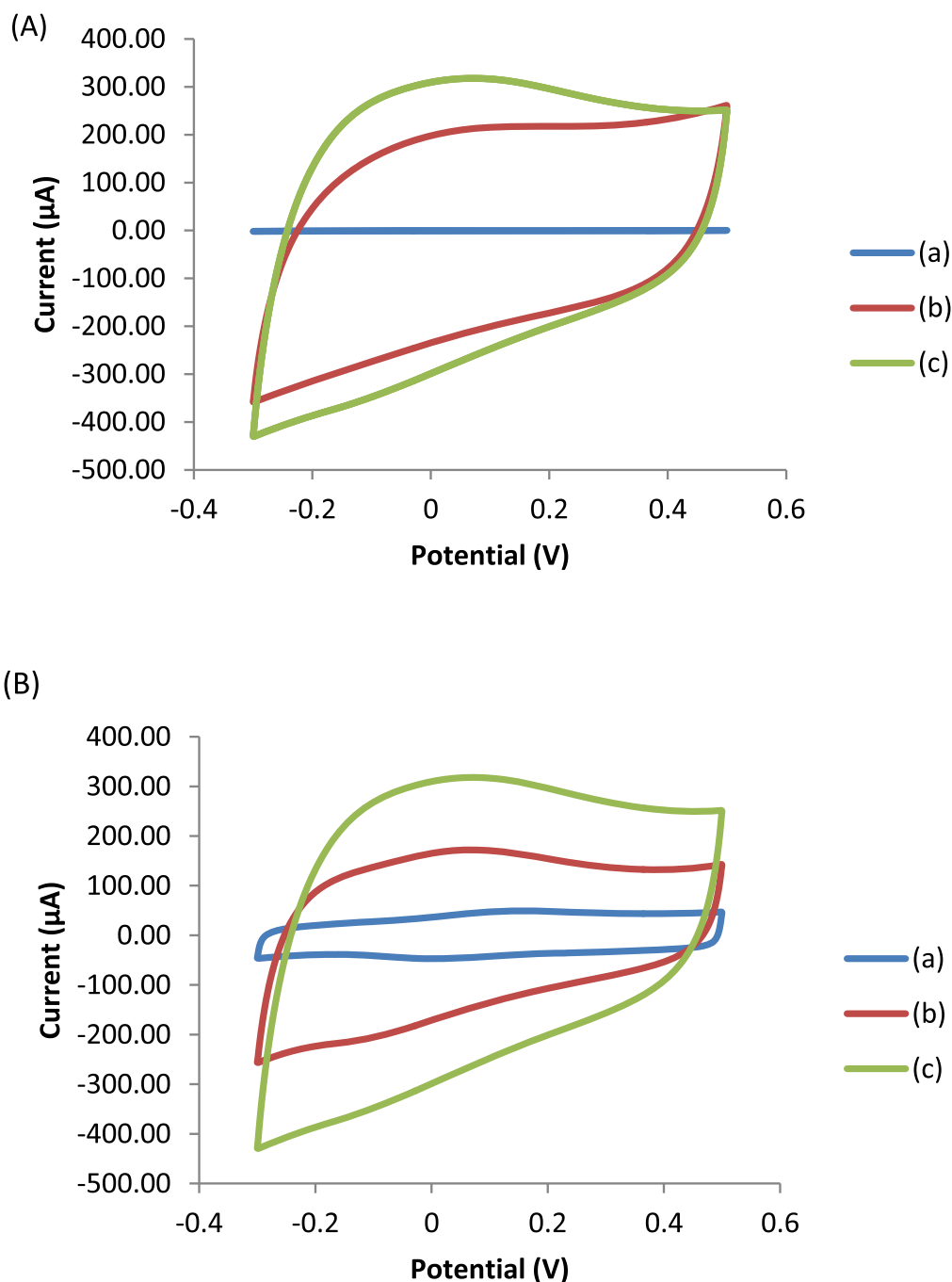


**Figure 7.** (A) Cyclic voltammogram showing Polythionine/PEDOT film following deposition from solution containing 10 mM thionine, 15 mM EDOT, 10 mM LiClO<sub>4</sub> at scan rate 0.1 V.s<sup>-1</sup> vs Ag/AgCl at a SAC-Pt modified GCE electrode. (a) GCE, (b) GCE/SAC-Pt, (C) GCE/SAC-Pt/pTH-PEDOT,  $E_{p(ox)} = 0.0506$  V,  $E_{p(red)} = -0.1691$  V,  $\Delta E_p = 0.2197$  V. pTH-PEDOT surface coverage ( $\Gamma$ ) =  $5.68 \times 10^{-9}$  mol.cm<sup>-2</sup>. (B) Overlay plots of Polythionine/PEDOT following deposition from a solution containing 10 mM thionine, 15 mM EDOT, 10 mM LiClO<sub>4</sub> in the absence and presence of SAC and SAC-Pt (3 mg.ml<sup>-1</sup> in 1% Nafion<sup>®</sup> solution consisting of 3:1 water: IPA) at scan rate 0.1 V.s<sup>-1</sup> vs Ag/AgCl at a modified GCE. (a) GCE/pTH-PEDOT, (b) GCE/SAC/pTH-PEDOT and (c) GCE/SAC-Pt/pTH-PEDOT.

plots were 59.6 mV.pH<sup>-1</sup> and 35.3 mV.pH<sup>-1</sup> respectively) with  $pK_a$  of 4. Scan rate studies were performed for the Polythionine/PEDOT film at GCE and Pt electrodes and a linear correlation was obtained ( $I_p$  vs  $\nu$ ) indicating that the reaction was surface confined. Plots of Log  $I_p$  vs Log scan rate for Polythionine/PEDOT film at GCE and Pt resulted in slopes of 0.9056 and 0.97 (close to the ideal value of 1). Laviron plots resulted in  $\alpha = 0.43$  for the anodic process with apparent charge transfer rate constant  $k_s$  of  $1.35 \times 10^{-3}$  s.

An investigation into the effect of SAC and SAC-Pt modified electrodes on Polythionine/PEDOT film growth was performed with

both modifiers resulting in enhanced film deposition with significant increases in surface coverage for Polythionine/PEDOT observed with each modification step;  $3.91 \times 10^{-11}$  mol cm<sup>-2</sup> (bare SPE)  $5.39 \times 10^{-11}$  mol cm<sup>-2</sup> (SPE/SAC/pTH-PEDOT) and  $1.16 \times 10^{-10}$  mol cm<sup>-2</sup> (SPE/SAC-Pt/pTH-PEDOT). SEM/EDX analysis of SPE/SAC-Pt/pTH-PEDOT modified electrodes was performed to verify changes in surface morphology and elemental analysis changed with each modification step. The images and spectra obtained confirmed that the surface was successfully modified with SAC-Pt and Polythionine/PEDOT deposition was successfully

**Table I. Summary results for Polythionine/PEDOT film grown at GCE, Pt and SPE modified electrodes.**

Electrode	$E_{p(ox)}$ (V)	$E_{p(red)}$ (V)	$\Delta E_p$ (V)	$E_{1/2}$ (V)	Stability % decrease in electroactivity	Surface coverage ( $\text{mol.cm}^{-2}$ )
GCE	0.1549	-0.001	0.154	0.077	23%	$1.03 \times 10^{-9}$
GCE/SAC	0.0677	-0.1134	0.046	-0.023	21%	$2.22 \times 10^{-9}$
GCE/SAC-Pt	0.0619	-0.1220	0.060	-0.030	10%	$5.68 \times 10^{-9}$
Pt	0.1569	-0.002	0.154	0.077	32%	$5.90 \times 10^{-10}$
Pt/SAC	0.1110	-0.0947	0.016	0.008	24%	$1.12 \times 10^{-9}$
SPE	0.1522	-0.0998	0.0524	0.026	15%	$5.94 \times 10^{-12}$
SPE/SAC	0.1507	-0.1824	0.0317	-0.016	19%	$5.39 \times 10^{-11}$
SPE/SAC-Pt	0.1455	-0.1973	0.0518	-0.026	13%	$1.16 \times 10^{-10}$

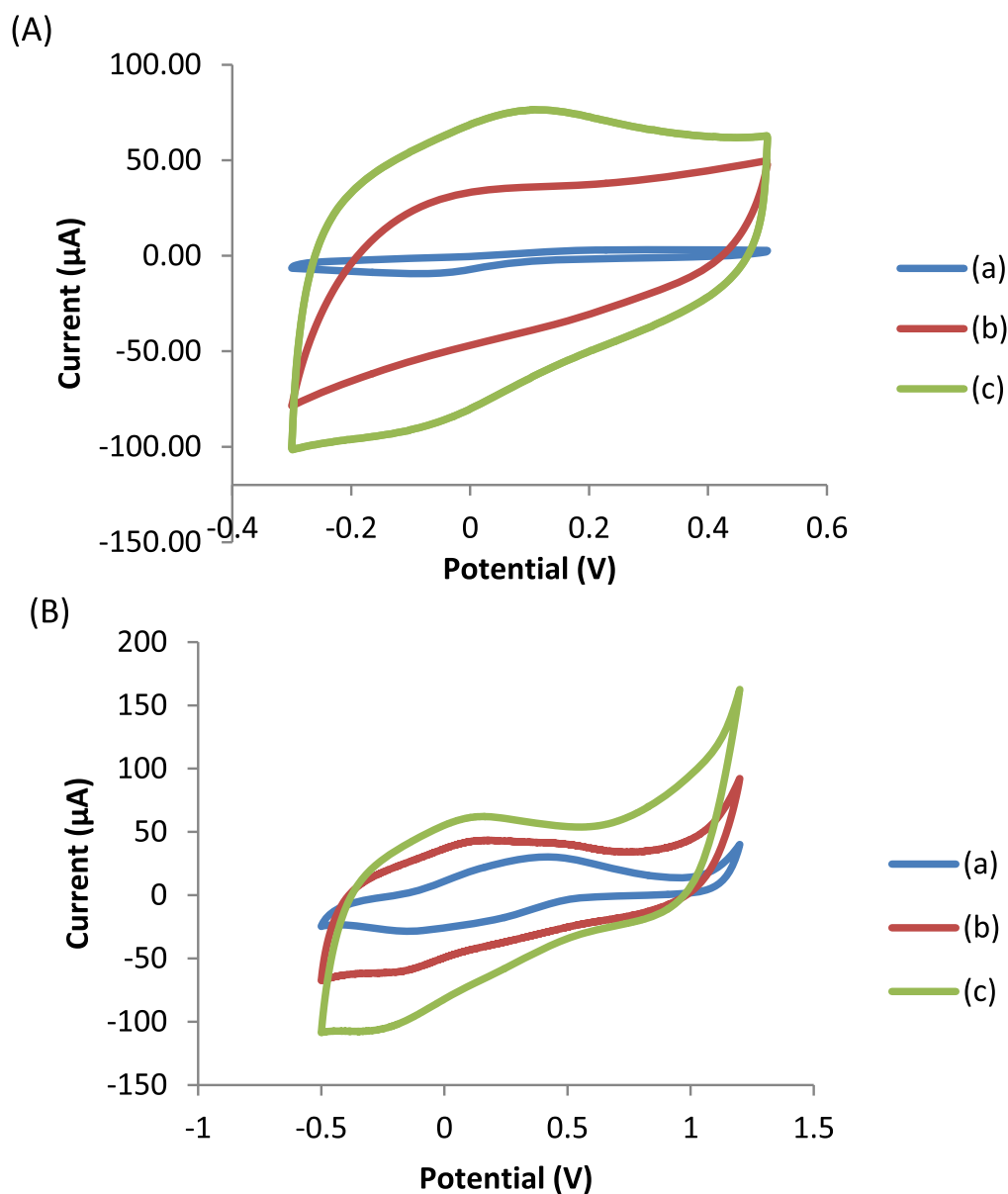
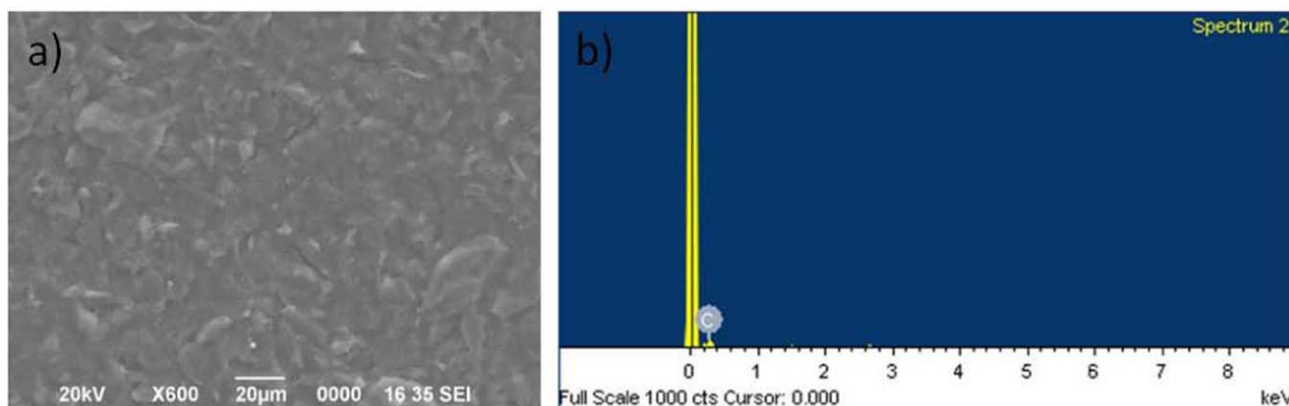
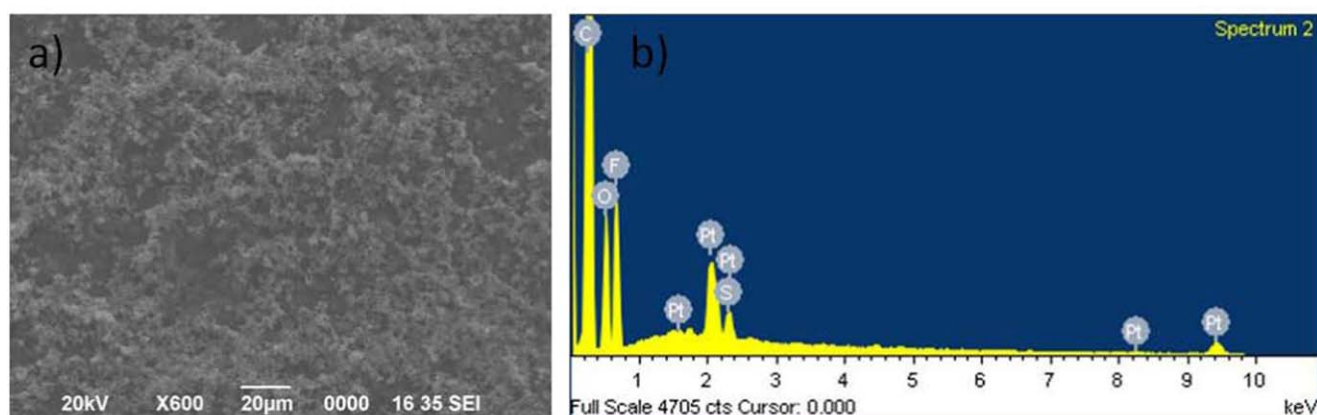


**Figure 8.** (A) Cyclic voltammogram showing Polythionine/PEDOT following deposition from solution containing 10 mM thionine, 15 mM EDOT, 10 mM  $\text{LiClO}_4$  at scan rate  $0.1 \text{ V.s}^{-1}$  vs Ag/AgCl at SAC modified Pt. (a) Bare Pt, (b) Pt/SAC, (c) Pt/SAC/pTH-PEDOT,  $E_{p(ox)} = 0.1006 \text{ V}$ ,  $E_{p(red)} = -0.1012 \text{ V}$ ,  $\Delta E_p = 0.2018 \text{ V}$ , pTH-PEDOT surface coverage ( $\Gamma$ ) =  $1.12 \times 10^{-9} \text{ mol.cm}^{-2}$ . (B) Overlay plots of Polythionine/PEDOT film following deposition from solution containing 10 mM thionine, 15 mM EDOT, 10 mM  $\text{LiClO}_4$  in the absence and presence of SAC and SAC-Pt ( $3 \text{ mg.mL}^{-1}$  in 1% Nafion<sup>®</sup> solution consisting of 3:1 water: IPA) at scan rate  $0.1 \text{ V.s}^{-1}$  vs Ag/AgCl at a modified SPE. (a) SPE/pTH-PEDOT, (b) SPE/SAC/pTH-PEDOT and (c) SPE/SAC-Pt/pTH-PEDOT.

(A)



(B)



(C)

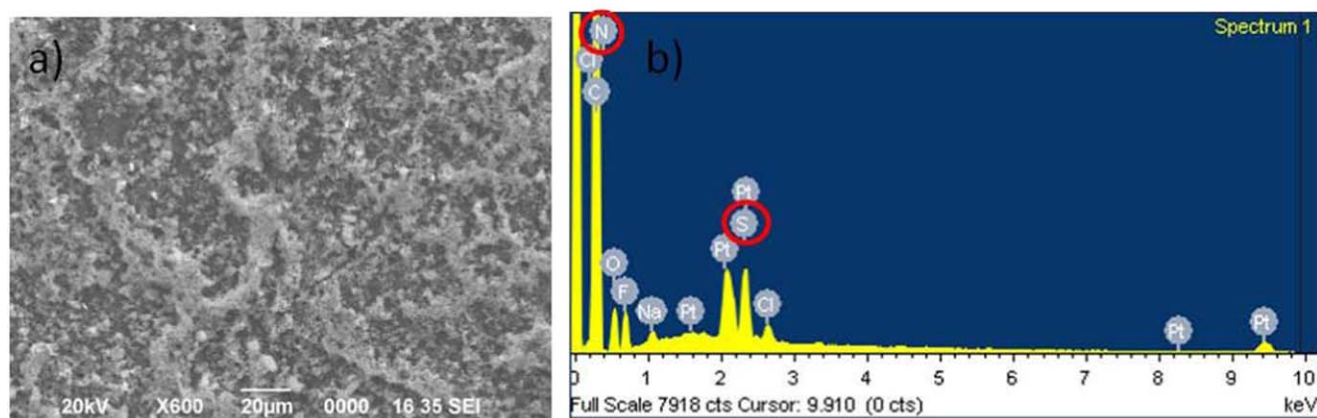


**Figure 9.** (A) SEM and EDX spectra for bare carbon SPE; (a) SEM image of bare SPE prior to modification, (b) EDX spectrum for the same showing peak for carbon. (B) SEM and EDX spectra for SPE/SAC-Pt modified electrode; (a) SEM image of SPE after SAC-Pt modification, (b) EDX spectrum for the same showing peaks for carbon, oxygen, fluorine, sulfur and platinum. (C) SEM and EDX spectra for SPE/SAC-Pt/pTH-PEDOT modified electrode (a) SEM image of SPE/SAC-Pt after modification with Polythionine/PEDOT b) EDX spectrum for the same showing peaks for carbon, oxygen, fluorine, sodium, platinum, sulfur and chlorine.

achieved. Finally, the contact angle of water was measured on SPE/pTH-PEDOT modified electrodes ( $68.30^\circ$  ( $n = 5$  S.D. 2.05)) concluding that the film had increased hydrophilicity relative to the unmodified carbon SPE surface ( $87.33^\circ$  ( $n = 5$ , S.D 3.28)).

### Acknowledgments

The authors would like to acknowledge the Technological University Dublin—Tallaght campus for President Research Award and funding (PPRA1501).

### References

- S. P. Massie, "The chemistry of phenothiazine." *Chem. Rev.*, **54**, 797 (1954).
- C. Bodea and I. Silberg, "Recent advances in the chemistry of phenothiazines." *Chim. Int. J. Chem.*, **66**, 321 (1968).
- G. Sudeshna and K. Parimal, "Multiple non-psychiatric effects of phenothiazines: a review." *Eur. J. Pharmacol.*, **648**, 6 (2010).
- G. Taurand, "Phenothiazine and derivatives." in *Ullmann's Encyclopedia of Industrial Chemistry* (Wiley-VCH Verlag GmbH & Co. KgaA, Weinheim, Germany) (2000).
- D. C. Le, C. J. Morin, M. Beljean, A. M. Siouffi, and P. L. Desbène, "Electrophoretic separations of twelve phenothiazines and N-demethyl derivatives by using capillary zone electrophoresis and micellar electrokinetic chromatography with non ionic surfactant." *J. Chromatogr. A*, **1063**, 235 (2005).
- Z. Li et al., "Amperometric biosensor for NADH and ethanol based on electro-reduced graphene oxide-polythionine nanocomposite film." *Sens. Actuators. B*, **181**, 280 (2013).
- C. Zhao, Z. Jiang, X. Cai, L. Lin, X. Lin, and S. Weng, "Ultrasensitive and reliable dopamine sensor based on polythionine/AuNPs composites." *J. Electroanal. Chem.*, **748**, 16 (2015).
- M. Yang, M. Guo, Y. Feng, Y. Lei, Y. Cao, D. Zhu, Y. Yu, and L. Ding, "Sensitive voltammetric detection of metronidazole based on three-dimensional graphene-like carbon architecture/polythionine modified glassy carbon electrode sensors." *J. Electrochem. Soc.*, **165**, B530 (2018).
- M. M. Rahman, J. Young Kim, and J.-J. Lee, "Label-free detection of DNA hybridization by using charge perturbation on poly(thionine)-modified glassy carbon and gold electrodes, sensors." *J. Electrochem. Soc.*, **162**, B159 (2015).
- A. A. Karyakin, E. E. Karyakina, and H.-L. Schmidt, "Electropolymerized azines: a new group of electroactive polymers." *Electroanalysis*, **11**, 149 (1999).
- E. Dempsey, D. Diamond, and A. Collier, "Development of a biosensor for endocrine disrupting compounds based on tyrosinase entrapped within a poly (Thionine) film." *Biosens. Bioelectron.*, **20**, 367 (2004).
- C. Chen, X. Hong, T. Xu, L. Lu, and Y. Gao, "Electrosynthesis and electrochemical and electrochromic properties of poly(aniline-co-N-methylthionine), organic and bioelectrochemistry." *J. Electrochem. Soc.*, **162**, G54 (2015).
- C. Chen, T. Xu, A. Chen, L. Lu, and Y. Gao, "Electrosynthesis of Poly(N-methylthionine)/polyaniline nanocomposites with enhanced electrochemical and electrocatalytic activities, organic and bioelectrochemistry." *J. Electrochem. Soc.*, **163**, G159 (2016).
- B. Hu, C.-Y. Li, J.-W. Chu, Z.-C. Liu, X.-L. Zhang, and L. Jin, "Electrochemical and electrochromic properties of polymers based on 2,5-di(2-thienyl)-1H-pyrrole and different phenothiazine unit, physical and analytical electrochemistry, electrocatalysis, and photoelectrochemistry." *J. Electrochem. Soc.*, **166**, H1 (2019).
- A. Peramo, M. G. Urbanek, S. A. Spanninga, L. K. Povlich, P. Cederna, and D. C. Martin, "In situ polymerization of a conductive polymer in acellular muscle tissue constructs." *Tissue Eng. Part A*, **14**, 423 (2008).
- G. Kaur, R. Adhikari, P. Cass, M. Bown, and P. Gunatillake, "Electrically conductive polymers and composites for biomedical applications." *RSC Adv.*, **5**, 37553 (2015).
- Y. Wu, Y. Yang, W. Lei, C. Li, Q. Hao, C. Zhang, Y. Zhang, and J. Su, "A facile construction of porous g-C<sub>3</sub>N<sub>4</sub>/poly(3,4-ethylenedioxythiophene) composite modified electrode for ascorbic acid determination sensors." *J. Electrochem. Soc.*, **165**, B118 (2018).
- S. Dash and N. Munichandraiah, "High catalytic activity of Au-PEDOT nano-flowers toward electrooxidation of glucose, physical and analytical electrochemistry, electrocatalysis, and photoelectrochemistry." *J. Electrochem. Soc.*, **160**, H858 (2013).
- K. Qu, Y. Bai, X. Liu, M. Deng, L. Wu, and Z. Chen, "Electro-catalytic behaviour of multiwall carbon nanotube-doped poly (3,4-ethylenedioxythiophene) toward environmental pollutant Bisphenol A, physical and analytical electrochemistry, electrocatalysis, and photoelectrochemistry." *J. Electrochem. Soc.*, **166**, H810 (2019).
- S. Warren, G. Munteanu, D. Rathod, T. McCormac, and E. Dempsey, "Scanning electrochemical microscopy imaging of poly (3,4-ethylenedioxythiophene)/thionine electrodes for lactate detection via NADH electrocatalysis." *Biosens. Bioelectron.*, **137**, 15 (2019).
- S. Warren, D. Rathod, T. McCormac, and E. Dempsey, "Investigations into the use of a thionine/PEDOT layer as an NADH electrocatalyst with applications in glutamate sensing." *ECS Trans.*, **25**, 21 (2010).
- S. Li, K. Han, J. Li, M. Li, and C. Lu, "Preparation and characterization of super activated carbon produced from gulfweed by KOH activation." *Micropor. Mesopor. Mater.*, **243**, 291 (2017).
- G. G. Stavropoulos, "Precursor materials suitability for super activated carbons production." *Fuel Process. Technol.*, **86**, 1165 (2005).
- F. Rouquerol, J. Rouquerol, and K. Sing, "Properties of some novel adsorbents." in *Adsorption by Powders and Porous Solids* (Elsevier, Amsterdam) p. 401 (1999).
- K. Xia, J. Hu, and J. Jiang, "Enhanced room-temperature hydrogen storage in super-activated carbons: the role of porosity development by activation." *Appl. Surf. Sci.*, **315**, 261 (2014).
- B. Singh, L. Murad, F. Laffir, C. Dickinson, and E. Dempsey, "Pt based nanocomposites (mono/bi/tri-metallic) decorated using different carbon supports for methanol electro-oxidation in acidic and basic media." *Nanoscale*, **3**, 3334 (2011).
- B. Meryemoglu, S. Irmak, A. Hasanoglu, O. Erbatur, and B. Kaya, "Influence of particle size of support on reforming activity and selectivity of activated carbon supported platinum catalyst in APR." *Fuel*, **134**, 354 (2014).
- M. M. Bruno, F. A. Viva, M. A. Petrucelli, and H. R. Corti, "Platinum supported on mesoporous carbon as cathode catalyst for direct methanol fuel cells." *J. Power Sources*, **278**, 458 (2015).
- A. Hayat and J. L. Marty, "Disposable screen printed electrochemical sensors: tools for environmental monitoring." *Sensors (Switzerland)*, **14**, 10432 (2014).
- V. C. Ferreira and O. C. Monteiro, "Synthesis and properties of Polythionine/Co-doped titanate nanotube hybrid materials." *Electrochim. Acta*, **113**, 817 (2013).
- A. S. N. Murthy and K. S. Reddy, "Cyclic-voltammetric studies of some phenothiazine dyes." *J. Chem. Soc. Faraday Trans. 1 Phys. Chem. Condens. Phases*, **80**, 2745 (1984).
- M. Fabretto, K. Zuber, C. Hall, P. Murphy, and H. J. Griesser, "The role of water in the synthesis and performance of vapour phase polymerised PEDOT electrochromic devices." *J. Mater. Chem.*, **19**, 7871 (2009).
- Y. Sun, Y. Bai, W. Yang, and C. Sun, "Controlled multilayer films of sulfonate-capped gold nanoparticles/thionine used for construction of a reagentless bienzymatic glucose biosensor." *Electrochim. Acta*, **52**, 7352 (2007).
- H. Hammani, W. Boumya, F. Laghrib, A. Farahi, S. Lahrach, A. Aboulkas, and M. A. El Mhammedi, "Electrocatalytic effect of NiO supported onto activated carbon in oxidizing phenol at graphite electrode: application in tap water and olive oil samples." *J. Assoc. Arab Univ. Basic Appl. Sci.*, **24**, 26 (2017).